BRIEF REPORT

Analytical exploration of the Mycenaean glass world via micro-PIXE: a contribution to our knowledge of LBA glass technology

M. Kaparou[1] · K. Tsampa[1] · N. Zacharias[2] · A. G. Karydas[1]

Abstract

During the Late Bronze Age, the Peloponnese with its palatial centers becomes the heartland of the Mycenaean world, resulting in an idiosyncratic material culture within the archaeological record, with glass constituting undoubtedly an important agent gaining prominence from the 15th cent. BC onwards, at the time when the palaces start rising and turning out to be characteristic to the Mycenaean material culture of the palatial elite. In this paper, the chemical composition of eleven (11) glass beads and relief plaques from three tombs of the necropolis in the area of Palaia Epidavros, Argolid in Greece have been studied to discuss aspects related to the nature of technology and provenance of fifteenth to eleventh century BC dated Mycenaean glass jewelry. The study resulted in the chemical fingerprinting of the collection by means of micro-PIXE succeeding in highlighting interesting technological aspects and assigning a likely origin of the studied samples. Importantly, since part of the assemblage had been studied in the past with the application of SEM–EDS and pXRF, the use of mPIXE enabled an enhanced discussion on glass related topics by comparing the results obtained.

Keywords Mycenaean glass world · Micro-PIXE · LBA glass technology

Introduction

In the Late Bronze Age LHI and LHII, the Argolid in northeast Peloponnese constitutes the geographic epicenter of the Mycenaean world on the Greek mainland with three citadels, at least three stately palaces, elaborate royal tombs and imposing cyclopean fortifications. In the Mycenaean Palatial Period, LHIIIA, and LHIIIB (1400–1190 BCE), the emerging palatial elite held authority over administrative and religious affairs, as well as production, trade, and storage of goods. The archaeological evidence supports the presence of a hierarchical structured society (Shelmerdine 2008), as for example the vast palatial centers in Mycenae, Tiryns, Pylos, and Thebes. It is also apparent in the archaeological record with the Mycenaean cultural impact going as far as the coast of Asia Minor and Northern Greece, while robust evidence of trade relations connects the region to Cyprus, further on the Near East, alongside central Mediterranean and the Balkans (Voutsaki 2010). While the Mycenaean glass artifacts support the presence of an individual glass industry with distinct characteristics, the absence of industrial debris, alongside the analytical data to date, suggests that solely secondary production took place in the Aegean. Thus, from an archaeological point of view, we can say quite safely that the glass technology and its specifics were transferred to the Aegean from Mesopotamia and Egypt, where an established technological base was already raising and raw glass was imported. The Mycenaean artisans would perform glass working, alongside other materials, such as gold and ivory, likely in the same area (Bennet 2008).

The eleven samples chosen for this study originate from burial contexts from the area of Palaia Epidavros, whose necropolis was in use from the fifteenth to the eleventh century BC (Archaeologikon Deltion, 1994). While the Mycenaean settlement of Palaia Epidavros, to which the necropolis belonged, is not yet located, its geographical position close to the Peloponnesian coast suggests a settlement prominent in maritime trade connecting the Mycenaean centers of the Argolid plain by sea. The majority of

✉ M. Kaparou
  kaparou@inp.demokritos.gr

1 Institute of Nuclear and Particle Physics, NCSR Demokritos, P. Grigoriou and Neapoleos 27, Aghia Paraskevi, Attiki, Greece

2 Department of History, Archaeology and Cultural Resources Management, University of the Peloponnese, 24133 Kalamata, Greece

the present glass fragments has been previously studied by means of SEM–EDS and pXRF analysis on an untreated surface. Conversely, the present micro-PIXE measurements aimed to generate a consistent data set of trace elements concentrations, aside from the major and minor constituents, on a polished surface of these glass fragments. In addition, the fast-scanning proton microprobe enabled the investigation of the spatial distribution of trace elements enlightening aspects of their provenance and mutual associations at the microscale.

Excavation works in the necropolis began towards the end of the nineteenth century on the steep eastern slope of Katarachi Hill, at Nera, west of the modern town of Epidavros. More recent excavations have revealed more parts of the necropolis, showing that it was organized into clusters of chamber tombs, cut into the natural bedrock of the area. As common for tombs of this type, the chamber tombs at Palaia Epidavros consist of a long doorway heading downwards with converging walls leading to a quadrilateral or circular chamber, having an opening sealed with bricks. They were used for multiple burials, possibly for members of the same family or dynasty, while pits discovered in the floor of the doorway and the chambers were used for additional burials. The deceased received burial gifts or "kterismata," commonly comprising clay vases, such as stirrup jars, small amphorae, alabastra, small boxes, beakers, and cups. The burials also regularly included clay figurines of the "phi" and "psi" type, copper weapons, stone seals, copper pins, spirals, beads, and tiles made of glass and faience, steatite buttons, and gold leaves (Archaeologikon Deltion 1994).

From a decorative point of view, the manufacturing techniques to produce glass artifacts in the Aegean, such as beads and relief plaques, appear to have developed from metalworking techniques (Nightingale 2008; Kaparou and Oikonomou 2022). Thus, decorative elements adopted for metalwork, such as thickened, ribbed borders, and granulation, became characteristic to Mycenaean glass beads. Almost all the glass of the Mycenaean period is colored with a range of colorants, including cobalt, copper, manganese, lead, and antimony (Kaczmarczyk and Hedges 1983).

Materials and methods

The glass samples

The studied artifacts derive from a cluster of four Mycenaean tombs (37°38′01.3″N 23°09′35.9″E), arranged in a row oriented from North to South. Samples were taken from all four tombs. Based on the burial gifts, tomb 1 dates to the LBAIIIB period. Tomb 2 is located 4 m south of tomb 1, while tomb 3 was discovered at 2.8 m south of tomb 2. Both tombs tomb 2 and tomb 3 are dated to the LBAII to the

LBAIIIA period on the basis of the finds and the welding of bronze vessels. Tomb 4 shares the same chronology with the latter (Archaeologikon Deltion 1994) (Appendix Table 3).

The samples constitute characteristic examples of the Mycenaean glass jewelry style, comprising both simple beads (4) and decorated relief plaques (7) in a deep blue or turquoise glass, when the hue is still visible, with 4 of them being opaque (Appendix Table 3). The selected samples are representative of the shapes and colors present in the broader assemblage. Eight of them (PE1, PE11, PE15, PE21, PE22, PE23, PE24, and PE25) have been previously published (Zacharias et al. 2018) using a combination of SEM–EDS, pXRF, and PGAA. The present measurements on those eight glass beads and relief plaques were implemented, because the former analysis was performed without sample preparation, due to permit restrictions. An additional aim was to overcome the analytical shortcomings of the previous analysis in the quantification of several trace elements by means of the pXRF analysis. The study focused on the applied raw materials, including the use of colorants and glassmaking technology. Provenance issues were not addressed. In the present study, a small part of 2×2 mm^2 was removed from each sample, embedded in epoxy resin and polished for analyses. The polishing of the glass surface was performed with abrasive paper of various grit sizes (1000, 1200, and 1500 μm).
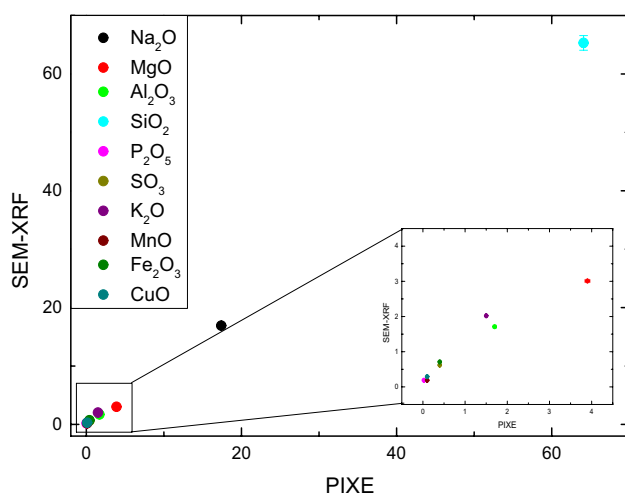
Micro-PIXE

The beads and relief plaques were investigated at the New AGLAE facility of the C2RMF in the Louvre Museum via external scanning micro-PIXE [Pichon et al. 2014; Lemasson et al. 2015; Bugoi et al. 2016]. The upgraded design and instrumentation integrated at the New AGLAE external Ion Beam Analysis station, which was funded by Equipex New-AGLAE ANR-10-EQPX22, allow the holistic examination of the artifacts surface, and thus, ~ few millimeter areas can be scrutinized within a reasonable time with micrometric spatial resolution (~ 40 μm) (Bugoi et al. 2020). PIXE suits ideally the compositional analysis of the glass matrix and in fingerprinting trace elements towards provenance assignment and studying the technological choices with respect to raw material selection (Calligaro 2008; Šmit et al. 2020). The scanning capabilities at the micrometer scale offer additional possibilities to evaluate the homogeneous distribution of different elements and identify insoluble inclusions. The data acquired via this technique—the first to date comprising micro-PIXE application on Mycenaean glass—formed a more accurate data set of the applied glass composition.

Scanning micro-PIXE was carried out using 3 MeV proton beam with ~ 3 nA beam current to investigate preselected areas (up to 2×2 mm^2) on the samples surface. AGLAE facility provides five Silicon Drift Detectors (SDD,

crystal area equal to 50 mm², 8 µm Be window), four with an appropriate filter (aluminum 50 µm) in front, to detect only medium- to high-energy X-rays (> 3 keV); however, in the present measurements, only three (#1, #3 and #4, HE-SDDs) of them were employed. For the detection of low-energy X-rays down to sodium, the fifth SDD (#0, LE-SDD) was used with the air path in front flushed with helium flow. The dose deposited on the samples was estimated at ~ 0.53 µC/ mm². For the scanning measurements, the step was selected equal to 10×10 µm (50×50 µm for the measurement of the reference glasses), whereas the pen size was set equal to 250 µm. The analysis of the cumulative spectra generated by the in-house software, TrauPIXE (Pichon et al. 2015) was carried out using the GUPIX software package (Campbell et al. 2010).

Four standards (BAM S-005 of the Federal Institute for Materials Research and Testing (BAM), Germany and Corning Archaeological Reference Glasses A/B/D by the Corning Museum of Glass (CMOG) (Adlington 2017)) were used to calibrate the instrumentation by determining the individual H factors for the LE-SDD and respective cumulative ones for the HE-SDDs. The reliability and accuracy of the mean H values exhibiting 5–10% relative uncertainties were evaluated by comparison of the determined concentrations versus the nominal ones for the set of the four reference glasses (Appendix Table 1). An excellent agreement can be generally observed with less than 10% difference for most elements in all four standards.

Concerning the comparison of the presently deduced concentrations with respect to the previously published ones, Fig. 1 shows the rather good correlation between SEM–EDS and the present µ-PIXE results, regarding the major and minor elem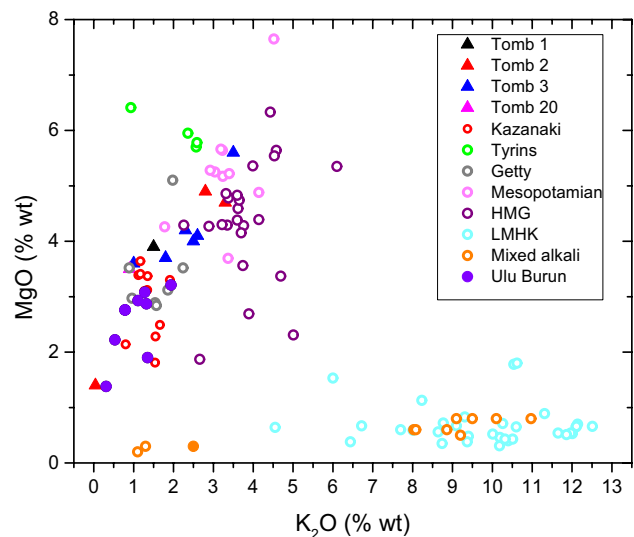ents. The comparison with the pXRF results is not shown since several trace elements were previously not quantified, due to limitations in the pXRF calibration.

Results and discussion

The concentrations for elements with atomic number $Z = 11–20$ are generated from the analysis of the LE-SDD spectra, while for those of $Z > 22$ the sum spectra of the HE-SDDs were used. Under the analytical protocol applied for the PIXE technique, the limits of detection (LoD) were determined for the major and several trace elements of interest and were normalized to 1 µC charge. The elemental concentrations which were found below the respective LoDs are not reported in the table of results (Appendix Table 2) for improved reliability of the reported concentrations.

As projected, all eleven samples appear to be soda-lime-silica glasses. Their levels of magnesia (av. 3.9% wt) and potash (av. 2% wt) (Fig. 2) suggest that they were made using plant ash as the alkali source and their compositions do not deviate from other LBA glass [SiO_2 (av. 68.4% wt), Al_2O_3 (av. 2.2% wt), Fe_2O_3 (av. 0.6% wt)]. Based on their magnesia levels (up to almost 6% wt) and their low potash levels, most samples could be characterized as high magnesium glasses (HMG). One sample (PE12) exhibits lower levels of both potash and magnesium, outlying from the rest, but this also exhibits very high silica levels of the order of almost 87%, suggesting leaching of certain elements and

Fig. 1 Comparison between SEM–EDS and µ-PIXE shows the rather good correlation, regarding the major and minor elements


Fig. 2 Correlation between magnesia and potash for the Palaia Epidavros assemblage compared to published Mycenaean equivalents, showing levels characteristic of plant ash glasses (data derived from Polikreti et al. 2011 (Pylos); Smirniou et al. 2012 (Kazanaki); Walton et al. 2009 (Tyrins, Getty); Henderson et al. 2015 (mixed alkali); Varberg et al. 2016 (Mesopotamian); Purowski et al. 2018 (HMG, LMHK); Lankton et al. 2022 (Ulu Burun))

enrichment in silica, due to the corrosion process it has undergone. Most samples from tomb 3 exhibit higher levels of potash, alongside two samples from tomb 2 falling close to the HGM group from Poland (Lankton et al. 2022). Sample PE27 from tomb 3 with lower potash levels coincides with a sample from Ulu Burun (mean concentration of 4 ingots) (reference), but it also exhibits high levels of silica (82.9% wt) and obvious signs of corrosion when studied microscopically.

The silica source would be expected to be quartz pebbles (Henderson 2013). It has been suggested that at least when it comes to relatively small-scale production, crushed and finely ground vein quartz pebbles were used as a source of silica, that being reinforced by the occurrence of the low alumina and trace element levels in the glasses of New Kingdom Egypt and Mesopotamia (Shortland et al. 2007; Rehren and Pusch 2008). Therefore, pure quartz pebbles constitute the most likely silica source, a choice that seems to be abandoned in later centuries and substituted by sand. The presence of high levels of Al_2O_3 (av. 2.2% wt) in this set of samples is not linked to the use of sand (Shortland et al. 2017)—which would be a rather rare incidence for the studied period—but at least for the cobalt-colored samples is rather due to the coloring of the glass by adding cobalt oxide, justifying high levels of alumina (more than 1.5%).

A SiO_2/Al_2O_3 vs TiO_2/Al_2O_3 biplot is useful, because these three oxides are related to sand as a silica source. Therefore, the correlation between these three oxides can highlight distinctive glassmaking regions via the use of different sands as previously demonstrated with 1st millennium AD glass (Phelps et al. 2016). In our case though, in which quartz must have been the primary silica source and not sand, a possible distinction based on these elements could suggest their introduction in a different way (Fig. 3). In using this correlation for the studied assemblage, the 6 samples from tomb 3 seem to form a different cluster with lower SiO_2/Al_2O_3 ratio in comparison to the rest. Most of these samples (5 out of 6) have been colored with the addition of cobalt and indeed most of them exhibit higher levels of the colorant (< 1000 ppm). They also match well with sample P15 from tomb 2, as in Fig. 2. These beads show no clear correlation with the Ulu Burun ingots; conversely, some correlation with the mixed alkali glasses from Frattesina is presented for most samples (Henderson et al. 2015).

Most samples are colored with the combination of cobalt oxide with contents between around 500 and 1200 ppm and cupric oxide varying from 0.1 to 0.5% wt indicating a deliberate addition of the copper colorant rather than contamination from the cobalt colorant. Three samples (PE11, PE12, PE27) instead were colored solely with the contribution of copper oxide (1.8, 0.52, and 1.15% wt respectively). PE11 has also been opacified with calcium antimonate crystals (Sb_2O_5 at 3.95% wt). Five samples from tomb 3 again outlie, whereas one
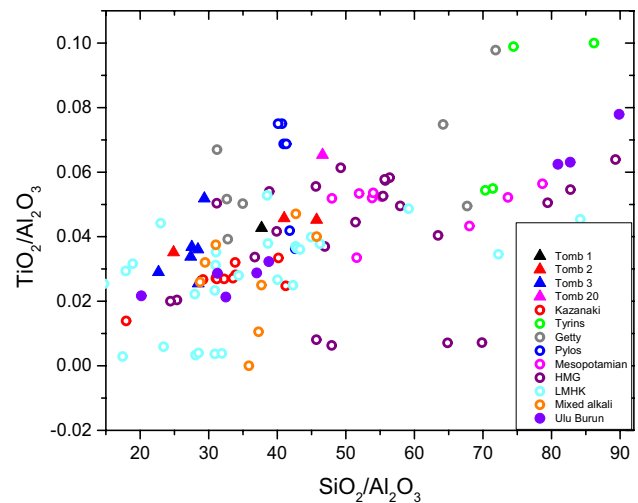

Fig. 3 The glass from Palaia Epidavros can be distinguished in two groups. The samples with lower SiO_2/Al_2O_3 ratio derive from tomb 3 and one sample from tomb 2 (data derived from Polikreti et al. 2011; Smirniou et al. 2012; Walton et al. 2009; Henderson et al. 2015; Varberg et al. 2016; Purowski et al. 2018; Lankton et al. 2022)
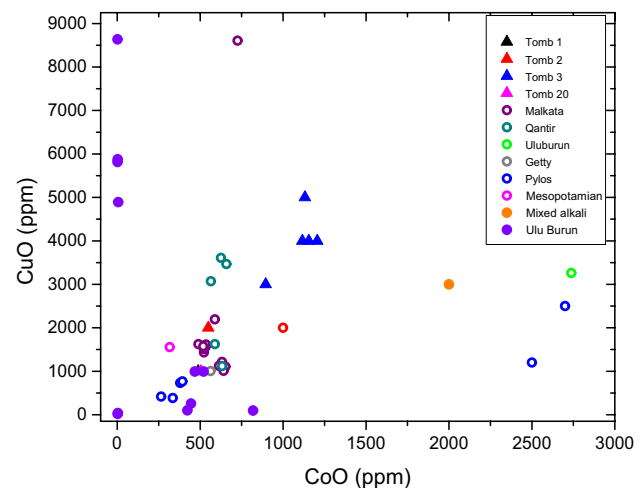
Fig. 4 Correlation of cobalt to copper oxides. Most samples have been colored with a combination of the two oxides, with only three samples with a characteristic turquoise color having been colored with the addition of cupric oxide. The tight subgroup of 4 samples derives from tomb 3 (data derived from Walton et al. 2009; Smirniou and Rehren 2013; Henderson et al. 2015; Varberg et al. 2016; Lankton et al. 2022)

sample from tomb 3 and one from tomb 2 correspond well with Ulu Burun ingots (Fig. 4). The acquisition of the elemental maps of glass sample PE24 with the HE-SDDs suggests that there is no correlation between this copper particle and the cobalt colorant, implying that the introduction of this cupric colorant occurred independently (Fig. 5). Smirniou and Rehren (2013) in their study of a broad set of data suggest that with respect to

Fig. 5 Copper and cobalt (top to bottom) elemental maps of glass sample PE24 acquired by "high" energy detectors. The pixel area is $40 \times 40 \ \mu m^2$ and the total scanned area of $0.5 \times 0.25 \ mm.^2$. The colorbar on the right shows the variation of the detected copper and cobalt intensity. The elemental maps were generated by PyMCA software (Solé et al. 2007)
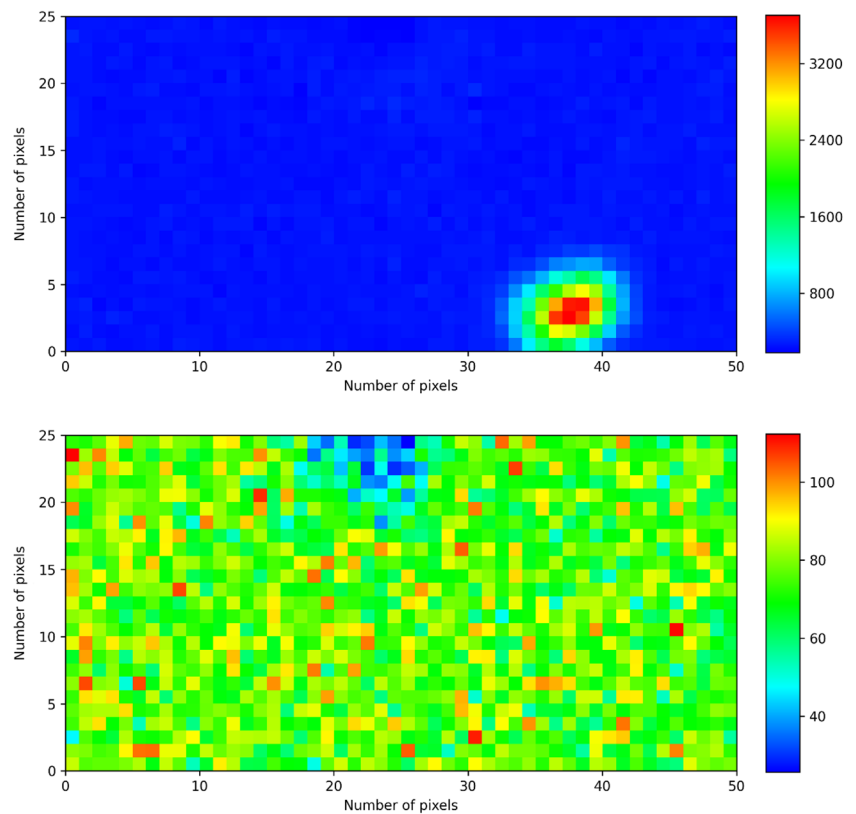
glasses colored with a combination of the two colorants, the likely explanation for the copper occurrence is related to the fact that copper is part of the suite of transition metals which are known to accompany cobalt in the alum deposits of the Egyptian Western Desert oases. Nevertheless, they also acknowledge the possibility that at least some of the copper originates from bronze vessels in which the colorant was prepared through a series of wet chemical steps. In comparing the average concentrations of the samples presented herein (Appendix Table 2), there are no significant differences with respect to elements associated with the base glass or regarding the somewhat elevated levels of Mn, Zn, and Ni, with As—elements related to cobalt in the alum deposits of the Egyptian Western Desert oases.
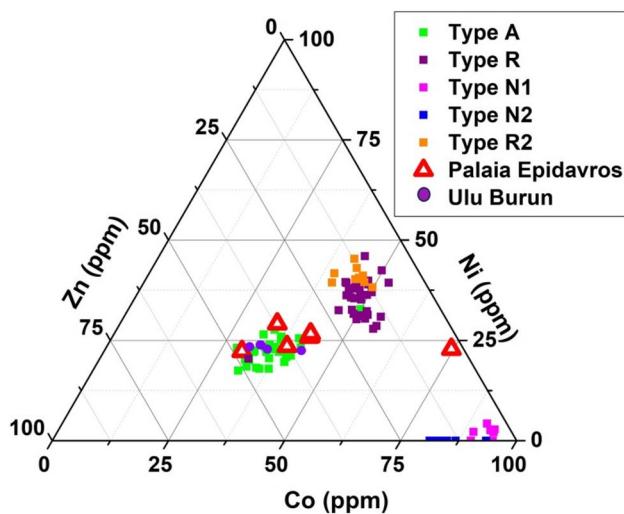
In samples from Palaia Epidavros tomb 3, the ratio of cobalt levels to the copper levels constitutes 1/3 or 1/4 of the respective. Nonetheless, the levels of potash are much higher than the usual low levels of potash for Mycenaean glass samples discussed in literature and for cobalt-colored glasses in general. Of course, low potash glass is not only found in cobalt-colored glass, but equally in various other colored glasses (Brill 1999; Shortland et al. 2006). As suggested in literature (Smirniou and Rehren 2013), low potash is not due to the colorant being added, but most likely it constitutes a feature of the base glass. The high levels of potash identified in this group of samples though could

suggest different possible reasons related to a plant ash with higher elevated levels of potash, e.g., the period of harvesting or the part of the plant used. It is clear though that low potash glass only occurs occasionally in the glass of this era.

An explanation for the occasional occurrence of unrelated cobalt-copper ratios could be that copper was added to weakly colored cobalt-blue glass to deepen the glass hue. This can be supported by the association of copper to tin which indicates the use of bronze or bronze scrap as colorant for samples PE22, 23, and 24, with Sn levels at 2779, 1569, and 1765 ppm respectively.

As expected for LBA cobalt-blue glasses, all the cobalt-containing glass beads yielded certain amounts of the accessory elements NiO, MnO, and ZnO, which are highly correlated to cobalt ore suggesting that these elements are connected to the source of the colorant (Fig. 6). With the alums from Dakhla and Kargha deposits in the Egyptian Western Desert oases as known source of cobalt in LBA, different types of cobalt colorants have been identified in literature (Abe et al. 2012). To assess, the provenance of the cobalt colorant of the Argolid samples, the cobalt-containing glasses were compared to published parallels representing different types of cobalt considered by Abe et al. (2012). As suggested by the ternary diagram (Fig. 6), most samples coincide with type A, with only two outliers, as well as with the cobalt-colored ingots form the Ulu

Fig. 6 Most samples from Palaia Epidavros coincide with type A and the cobalt-colored Ulu Burun ingots, the traditional colorant used in the 18th Dynasty (Abe et al. 2012; Lankton et al. 2022)
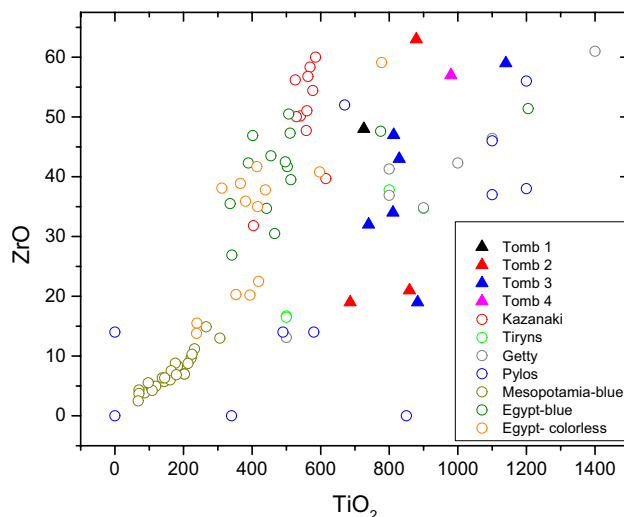
Fig. 7 Egyptian glass is most frequently linked to elevated contents of TiO$_2$ and ZrO (up to almost 80 ppm) and all the Argolid samples tend to have higher titania levels and equally high zirconium of more than 30 ppm, with the exception of three samples (data derived from Polikreti et al. 2011, Smirniou et al. 2012, Walton et al. 2009, Shortland et al. 2007)

Burlun shipwreck analyzed by Lankton et al. (2022). Type A, a colorant used during the eighteenth Dynasty, is characterized by the variety of transition metals as impurities originating from the cobaltiferous alums from the Western Desert Oases in Egypt.

Trace element analysis has been able to identify regionally diagnostic markers that enable us to differentiate between Mesopotamian and Egyptian glass (Shortland et al. 2007). Several elements associated with the

raw materials have been seen to be distinct enough to chemically discriminate glasses from these two major glassmaking centers of the LBA. Egyptian glass is most frequently linked to elevated contents of Ti and Zr, whereas all known Mesopotamian and some non-cobalt Mycenaean glasses tend to have lower Ti levels and less than 20 ppm Zr (Shortland et al. 2007). All the Argolid samples tend to have higher titania levels and equally high zirconium of more than 30 ppm, except for two samples (Fig. 7).

The results of the study of the eleven samples from the area of Palaia Epidavros in Argolid suggest a likely Egyptian origin. Most samples from tomb 3 do seem to exhibit the result of a different set of technological choices. Four samples from this set also have higher levels of potash, and in general, they seem to cluster when compared forming a subgroup within the assemblage. Another interesting technological outcome from the present analysis is the assertion that copper is not related to cobalt and that copper has entered the glass independently and not through mixing or recycling.

The samples from tombs 2 and 3 with higher potash can be representative of a different plant ash used, obviously richer in potash, or different choices related to plant harvesting, area of harvesting, etc. According to our current knowledge, raw glass was imported in the Aegean, but the specifics of this import are not yet clear. Whether this glass was simply remelted to form objects or the batch was somehow enriched in the local workshops, for instance in colorants, based on the desired outcome, is not absolutely clear. More data is needed towards compiling a more complete picture of the production and consumption of glass during LBA in the Aegean. Nevertheless, differences in glass production activities and consumption within the Mycenaean world have been observed, even between close-by sites such as Mycenae.

Such differences as the ones noted in the assemblage could be characteristic of certain micro-traditions and/or a different positioning of a social group within a broader set of trends or old customs. According to the data collected, the glass beads and plaques from Palaia Epidavros derive from Egypt. This is attested both by the cobalt colorant used to color most of the samples and their trace elements analysis (Ti-Zr). Nevertheless, as suggested earlier, most samples from tomb 3 do seem to form a rather tight cluster which could allow for a discussion of a different production center or different technological choices which could be also made locally. Given the very small amount of data, the exact character of the latter is not assured; hence, only hypotheses can be made based on the knowledge acquired so far.

If the case is that some kind of treatment of the batch was performed at the secondary stage of production, some considerations shall be taken into account. As suggested by

Voutsaki (2021), the Mycenaean world was not a uniform showing divergent individualities, and of course, Mycenae itself is not representative for the entire "Mycenaean world" that shared similar features characterizing a generalized "Mycenaean" identity. Various communities and their constituent social groups positioned themselves differently, either aligning with established traditions or embracing emerging trends. How glassworkers positioned themselves within the centralized model at the time is not clear. While most probably a certain process of raw glass procurement would have been maintained, given the secondary nature of the activity, this cannot exclude the interventions of local artisans as human actors in manipulating the material. A noteworthy technological result arising from the current analytical study is that there is no correlation between copper and cobalt. Additionally, the study suggests that copper has independently entered the glass, rather than through a process of mixing or recycling. This could constitute evidence of reworking of the batch at a later stage, even at the secondary workshop. Given this, we cannot exclude other forms of intervention, which could for instance explain the somehow unique signature especially of the samples from tomb 3. At present, we cannot address the nature of the latter, as we cannot exclude that this glass was imported as such. More data will help answer this query.

Conclusions

This is the first study presenting Mycenaean glass data with the application of external scanning micro-PIXE. The chemical analysis of the glass offered herein is in general concurring with what would have been expected for LBA glass, in terms of the glass composition and a likely Egyptian origin. Apart from three samples which could have been colored with copper as a colorant (with PE12 and PE27 being corroded), most of the samples were colored using a combination of cobalt oxide and cupric oxide. The identification of an independent copper particle alongside with the higher levels of arsenic and lead could suggest that copper was added independently, as it does not seem to be related to intentional mixing or recycling, but it could be associated to the desire to influence the cobalt color hue with the addition of copper. The analysis revealed that samples from tomb 3 exhibited a different pattern, forming a rather tight subgroup within the broader set of data and likely representing a different technology than the rest of the samples. Some of the latter have higher potash levels than usual for this era, which at present is not fully understood but might be explained by adding ashes to the batch. Overall, this set of data contributes additional information to the current chemical and technological knowledge of LBA glass in the Aegean.

Appendix

Table 1 Analyses of BAM and Corning A, B, and D, compared to nominal values

		BAM		Corning A		Corning B		Corning D	
		Nominal	Measured	Nominal	Measured	Nominal	Measured	Nominal	Measured
Na_2O	%wt	13.7	13.1	14.3	13.0	17.0	16.5	1.20	1.39
MgO	%wt	2.30	2.09	2.66	2.72	1.03	1.03	3.94	4.18
Al_2O_3	%wt	1.10	1.15	1.00	0.99	4.36	4.28	5.30	5.16
SiO_2	%wt	71.00	66.87	66.56	67.99	61.55	63.23	55.24	55.82
P_2O_5	%wt			0.0847	0.0555	0.82	0.80	3.93	4.03
SO_3	%wt	0.19	0.20	0.14	0.17	0.49	0.57	0.23	0.25
K_2O	%wt	0.70	0.65	2.87	2.89	1.00	1.04	11.3	11.7
CaO	%wt	10.5	10.8	5.03	4.99	8.56	8.65	14.8	14.3
TiO_2	%wt	0.0163	0.0193	0.79	0.78	0.09	0.10	0.38	0.38
MnO	%wt	0.0124	0.0128	1.00	1.02	0.25	0.24	0.55	0.55
Fe_2O_3	%wt	0.0422	0.0436	1.09	1.09	0.34	0.34	0.52	0.50
CoO	ppm	49	56	1700	1743	460	448	230	196
NiO	ppm	59	64	200	242	990	968	500	491
CuO	%wt	0.0112	0.0112	1.17	1.19	2.66	2.72	0.38	0.37
ZnO	ppm	203	210	440	453	1900	1875	1000	945
As_2O_3	ppm	132	130						
SrO	ppm	151	158	1000	1037	190	187	570	550
ZrO_2	ppm	842	827	50	69	250	258	125	117
SnO_2	ppm	106	LoD	2021	2074	426	314	1064	1063
Sb_2O_5	ppm	132	LoD	17,500	17,836	4600	4584	9700	9548
PbO	ppm	202	232	725	814	6100	5147	2410	2443

Table 2 Compositional analysis of the Palaia Epidavros glass samples by scanning micro-PIXE. The relative uncertainties are calculated by the expanded uncertainty formula which includes the fit element principal peak areas, the fit error, and the empirical statistical error. Limits of detection (LoD) expressed in parts per million (ppm) for main and trace elements in glass matrix for $Q = 1$ µC. LoD for the elements Na to Ca is generated from the analysis of the LE-SDD spectra, while for elements of higher atomic number, the sum spectra of the HE-SDDs were used

		PE1	Σ%	PE11	Σ%	PE12	Σ%	PE15	Σ%	PE21	Σ%	PE22	Σ%	LoD [ppm]
Na$_2$O	% wt	17.4	0.8	14.7	1.4	0.1	24.5	15.9	1.0	15.9	0.9	16	1.0	484
MgO	% wt	3.9	1.4	4.9	1.8	1.4	1.6	4.7	1.6	4.1	1.4	5.6	1.2	377
Al$_2$O$_3$	% wt	1.7	2.0	1.5	3.3	1.9	1.3	2.5	2.0	2.3	1.6	2.8	1.5	313
SiO$_2$	% wt	64.1	0.4	61.5	0.5	86.9	0.4	62.2	0.5	65.4	0.4	63.5	0.4	200
P$_2$O$_5$	% wt	LoD	-	LoD	-	0.2	10.3	LoD	-	LoD	-	0.6	15	229
SO$_3$	% wt	0.4	3.8	0.6	4.5	0.2	4.5	0.5	3.5	0.5	4	0.4	4.0	227
K$_2$O	% wt	1.5	0.9	2.8	1.1	0.04	12	3.3	0.9	2.6	0.8	3.5	0.7	94
CaO	% wt	8.8	0.5	7.7	1.0	3.3	1.0	7.2	0.7	6.5	0.6	5.7	0.6	96
TiO$_2$	% wt	0.1	3.0	0.1	10	0.1	6.0	0.1	2.8	0.1	3.2	0.1	3.0	34
MnO	% wt	0.1	1.0	0.1	2.5	0.01	2.1	0.1	1.1	0.1	1.0	0.04	1.6	6
Fe$_2$O$_3$	% wt	0.4	0.8	0.5	1.2	0.6	0.7	0.6	0.8	0.6	0.8	0.6	0.7	6
CoO	ppm	488	2.4	LoD	-	LoD	-	549	2.5	1155	1.6	1206	1.5	4
NiO	ppm	366	1.4	276	3.0	71	2.2	LoD	-	705	1.3	369	1.7	3
CuO	% wt	0.1	1.1	1.8	1.0	0.5	0.7	0.2	0.8	0.4	0.8	0.4	0.7	2
ZnO	ppm	789	1.0	LoD	-	55	14	527	1.4	854	1.3	43	11	2
As$_2$O$_3$	ppm	6	16	166	4.0	24	5.3	LoD	-	45	16	69	19	3
SrO	ppm	1557	1.3	1171	3.0	122	3.8	1422	1.5	945	2.0	777	1.9	3
ZrO	ppm	48	19	LoD	-	21	14	63	19	43	18	47	20	19
Sn	ppm	LoD	-	61	8.0	124	3.5	LoD	-	LoD	-	2779	1.0	190
Sb$_2$O$_5$	ppm	LoD	-	39487	4.0	LoD	-	LoD	-	LoD	-	LoD	-	340
PbO	ppm	LoD	-	94	7.0	62	6	LoD	-	3251	0.1	LoD	-	10
		PE23	Σ%	PE24	Σ%	PE25	Σ%	Pe27	Σ%	PE35	Σ%	LoD [ppm]		
Na$_2$O	% wt	15.9	1.0	15.7	1.2	16.6	0.9	3.9	1.7	12.9	1.1	484		
MgO	% wt	4.2	1.3	4.0	1.9	3.7	1.5	3.6	1.3	3.5	1.8	377		
Al$_2$O$_3$	% wt	2.4	1.4	2.4	2.1	2.2	1.7	2.9	1.4	1.5	2.4	313		
SiO$_2$	% wt	65.7	0.4	66.1	0.7	64.6	0.4	82.6	0.4	69.9	0.5	200		
P$_2$O$_5$	% wt	0.1	18	LoD	-	LoD	-	LoD	-	LoD	-	229		
SO$_3$	% wt	0.5	4.4	0.5	5.1	0.5	3.6	0.3	5.2	0.4	5.7	227		
K$_2$O	% wt	2.3	0.7	2.5	1.0	1.8	0.9	1.0	1.2	0.9	1.6	94		
CaO	% wt	6.5	0.7	6.4	0.9	7.9	0.5	3.1	0.7	8.5	0.6	96		
TiO$_2$	% wt	0.1	3.6	0.1	4	0.1	2.5	0.1	3.2	0.1	3.2	34		
MnO	% wt	0.1	1.1	0.1	1.2	0.1	1.0	0.1	1.5	0.1	1.2	6		
Fe$_2$O$_3$	% wt	0.5	0.8	0.6	0.6	0.7	0.8	0.5	0.9	0.5	0.9	6		
CoO	ppm	1116	1.6	1132	1.7	895	2.1	LoD	-	505	2.8	4		
NiO	ppm	679	1.3	713	1.4	543	1.4	21	6.7	435	1.6	3		
CuO	% wt	0.4	0.8	0.5	0.6	0.3	0.8	1.2	0.9	0.1	1.0	2		
ZnO	ppm	835	1.4	830	1.6	870	1.2	LoD	-	551	1.5	2		
As$_2$O$_3$	ppm	40	17	45	14	21	20	LoD	6.7	LoD	-	3		
SrO	ppm	722	2	882	2.5	957	1.7	364	0.2	884	1.7	3		
ZrO	ppm	34	18	LoD	-	59	17.3	32	15.1	57	19	19		
Sn	ppm	1569	1.3	1765	1.6	LoD	-	LoD	-	LoD	-	-		
Sb$_2$O$_5$	ppm	LoD	-	LoD	-	1977	8.4	LoD	-	LoD	-	340		
PbO	ppm	1061	1.6	977	1.9	LoD	-	LoD	-	LoD	-	10		

Tables 1, 2 and 3

Table 3 Samples description and chronology

	Sample	Colour	Tomb	Dating (BCE)	Object (bead or plaque)	Photographic documentation
	PE1	TransparentDeep Blue	1	1330-1190	Plaque- double rosette	
	PE11	Opaque light blue	2	1600-1330	Bead- barrel shaped	
	PE12	Opaque light blue	2	1600-1330	Bead- barrel shaped	
	PE15	Transparent Deep Blue	2	1600-1330	Bead- cylindrical with bands	
	PE21	Transparent Deep Blue	3	1600-1330	Plaque- single volute hanging from bar	
	PE22	Transparent Deep Blue	3	1600-1330	Plaque- single volute hanging from bar	
	P23	Transparent Deep Blue	3	1600-1330	Plaque- ivy leaf	
	PE24	Transparent Deep Blue	3	1600-1330	Plaque- ivy leaf	
	PE25	Transparent Deep Blue	3	1600-1330	Plaque- ivy leaf	
	PE27	Transparent Deep Blue	3	1600-1330	Small round bead	
	PE35	Transparent Deep Blue	20	1600-1330	Plaque- suspended curl on plaque hanging from a bar	

Declarations

Competing interests The authors declare no competing interests.

References

Abe Y, Harimoto R, Kikugawa T, Yazawa K, Nishisaka A, Kawai N, Yoshimura S, Nakai I (2012) Transition in the use of cobalt-blue colorant in the New Kingdom of Egypt. J Archaeol Sci 39:1793–1808

Adlington L (2017) The Corning Archaeological Reference Glasses: new Values for "old" compositions, Papers from the Institute of Archaeology 27(1), Art. 2. https://doi.org/10.5334/pia-515

Archaeologikon Deltion 50 (1994) (Αρχαιολογικόν Δελτίον 50) pp. 156–158 (in Greek)

Bennet J 2008) Speculations on palatial production in Mycenaean Greece with (some) reference to glass. In: Jackson, C.M., and Wager, E.C., (eds.), Vitreous materials in the Late Bronze Age Aegean, Sheffield Studies in Archaeology 9, Oxford, pp. 151–172

Brill RH (1999) Chemical analyses of early glasses, vols. 1 (tables) and 2 (catalogue). Corning Museum of Glass, Corning, New York

Bugoi R, Poll I, Mănucu-Adameşteanu Gh, Calligaro T, Pichon L, Pacheco C (2016) PIXE-PIGE analyses of Byzantine glass bracelets (10th-13th centuries AD) from Isaccea. Romania J Radioanal Nucl Chem 307:1021–1036

Bugoi R, Măgureanu A, Măgureanu D, Lemasson Q (2020) IBA analyses on glass beads from the migration period. Nuclear Instruments and Methods in Physics Research, Section B: Beam Interactions with Materials and Atoms, 478 (November 2019), pp. 150–157. https://doi.org/10.1016/j.nimb.2020.05.025

Calligaro T (2008) PIXE in the study of archaeological and historical glass. X-Ray Spectrom 37:169–177

Campbell JL, Boyd NI, Grassi N, Bonnick P, Maxwell JA (2010) The Guelph PIXE software package IV. Nucl Instrum Methods Phys Res, Sect B 268(20):3356–3363. https://doi.org/10.1016/j.nimb.2010.07.012

Henderson J (2013) Ancient glass, an interdisciplinary exploration. Cambridge University Press, New York and Cambridge

Henderson J, Evans J, Bellintani P, Bietti-Sestieri A (2015) Production, mixing and provenance of Late Bronze Age mixed alkali glasses from northern Italy: An isotopic approach. J Archaeol Sci 55. https://doi.org/10.1016/j.jas.2014.12.006

Kaczmarczyk A, Hedges REM (1983) Ancient Egyptian Faience. An analytical survey of Egyptian Faience from Predynastic to Roman times, Warminster, Aris and Philips

Kaparou M, Oikonomou A (2022) Mycenaean through Hellenistic glass in Greece: where have we got to? Archaeol Anthropol Sci 14:92. https://doi.org/10.1007/s12520-022-01558-7

Lankton JW, Pulak C, Gratuze B (2022) Glass ingots from the Uluburun shipwreck: Addition of glass cullet during manufacture and evidence for the changing context of New Kingdom Egyptian glass production in the late 18th Dynasty. J Archaeol Sci: Reports 45. https://doi.org/10.1016/j.jasrep.2022.103596

Lemasson Q, Moignard B, Pacheco C, Pichon L, Guerra MF (2015) Fast mapping of gold jewellery from ancient Egypt with PIXE: searching for hard-solders and PGE inclusions. Talanta 143:279–286. https://doi.org/10.1016/j.talanta.2015.04.064

Nightingale G (2008) Tiny, fragile, common, precious. Mycenaean glass and faience, beads and other objects. In: Jackson CM, Wager E (eds) Vitreous material in the Late Bronze Age Aegean. Oxbow Books, Sheffield Studies in Aegean Archaeology, Oxford, p 9

Phelps M, Freestone IC, Gorin-Rosen Y, Gratuze B (2016) Natron glass production and supply in the late antique and early medieval Near East: the effect of the Byzantine-Islamic transition. J Archaeol Sci pp. 57–71

Pichon L, Moignard B, Lemasson Q, Pacheco C, Walter P (2014) Development of a multi-detector and a systematic imaging system on the AGLAE external beam, Nuclear Instruments and Methods in Physics Research Section B: Beam Interactions with Materials and Atoms, Volume 318. Part A. https://doi.org/10.1016/j.nimb.2013.06.065

Pichon L, Calligaro T, Lemasson Q, Moignard B, Pacheco C (2015) Programs for visualization, handling and quantification of PIXE maps at the AGLAE facility. Nucl Instrum Methods Phys Res, Sect B 363:48–54. https://doi.org/10.1016/j.nimb.2015.08.086

Polikreti K, Murphy JMA, Kantarelou V, Karydas AG (2011) XRF analysis of glass beads from the Mycenaean palace of Nestor at Pylos, Peloponnesus, Greece: new insight into the LBA glass trade. J Archaeol Sci 38:2889–2896

Purowski T, Kępa L, Wagner B (2018) Glass on the Amber Road: the chemical composition of glass beads from the Bronze Age in Poland. Archaeol Anthropol Sci 10:1283–1302. https://doi.org/10.1007/s12520-016-0443-8

Rehren, Th, Pusch, E (2008) Crushed rock and molten salt? Some aspects of the primary glass production at Qantir/Pi-Ramesse. In: Vitreous Materials in the Late Bronze Age Aegean, Edited by C. M. Jackson and E. C. Wager, Sheffield Studies in Aegean Archaeology, Oxbow pp. 14- 33

Shelmerdine CW (2008) Background. In: In Shelmerdine CW (ed) sources and methods. Age. Cambridge University Press, The Cambridge Companion to the Aegean Bronze, pp 1–8

Shortland A, Rogers N, Eremin K (2007) Trace element discriminants between Egyptian and Mesopotamian Late Bronze Age glasses. J Archaeol Sci 34:781–789

Shortland A, Tite MS, Ewart I (2006) Ancient exploitation and use of cobalt alums from the Western Oases of Egypt. Archaeometry 48, pp. 153 - 168. https://doi.org/10.1111/j.1475-4754.2006.00248.x

Shortland A, Kirk S, Eremin K, Degryse P, Walton M (2017) The analysis of Late Bronze Age glass from Nuzi and the question of the origin of glass-making. Archaeometry 60. https://doi.org/10.1111/arcm.12332

Smirniou M, Rehren Th, Adrymi-Sismani V, Asderaki-Tzoumerkioti E, Gratuze B (2012) Mycenaean beads from Kazanaki, Volos: a further node in the LBA glass network In: Ignatiadou, D. and Antonaras, A., (eds), Annales du 18e Congrès de l'Association Internationale pour l'Histoire du Verre, Thessaloniki 2009 pp. 11-18

Smirniou M, Rehren Th (2013) Shades of blue – cobalt-copper coloured blue glass from New Kingdom Egypt and the Mycenaean world: a matter of production or colourant source? J Archaeol Sci 40(12):4731–4743. https://doi.org/10.1016/j.jas.2013.06.029

Šmit Ž, Laharnar B, Turk P (2020) Analysis of prehistoric glass from Slovenia. J Archaeol Sci: Reports 29, https://doi.org/10.1016/j.jasrep.2019.102114.

Solé VA, Papillon E, Cotte M, Walter P, Susini J (2007) A multiplatform code for the analysis of energy-dispersive X-ray fluorescence spectra, Spectrochim. Acta - Part B at Spectrosc 62(1):63–68. https://doi.org/10.1016/j.sab.2006.12.002

Varberg J, Gratuze B, Kaul F, Haslund Hansen A, Rotea M, Wittenberger M (2016) Mesopotamian glass from Late Bronze Age Egypt, Romania, Germany and Denmark. J Archaeol Sci 74:184–194. https://doi.org/10.1016/j.jas.2016.04.010

Voutsaki S (2010) Argolid. In: Cline EH (ed) The Oxford handbook of the Bronze Age Aegean. Oxford University Press, Oxford, pp 599–613

Voutsaki S (2021) Social change and human agency: The Argolid at the onset of the Mycenaean era Birgitta Eder – Michaela Zavadil (eds.), (Social) Place and space in Early Mycenaean Greece, Denkschriften der phil.-hist. Klasse 528 Mykenische Studien 35 2021, Austrian Academy of Sciences Press, ISBN (printed edition) 9783700188544, ISBN (online edition) 978–3–7001–8934–3

Walton MS, Shortland AJ, Kirk S, Degryse P (2009) Evidence for the trade of Mesopotamian and Egyptian glass to Mycenaean Greece. J Archaeol Sci 36:1496–1503

Zacharias N, Kaparou M, Oikonomou A, Kasztovszky Z (2018) Mycenaean glass from the Argolid, Peloponnese, Greece: a technological and provenance study. Microchemistry J 141:404–417